International Journal of
Computing and
Engineering
(IJCE)

CFD Simulation of Steady, Compressible Flow around the Naca 2412 Airfoil

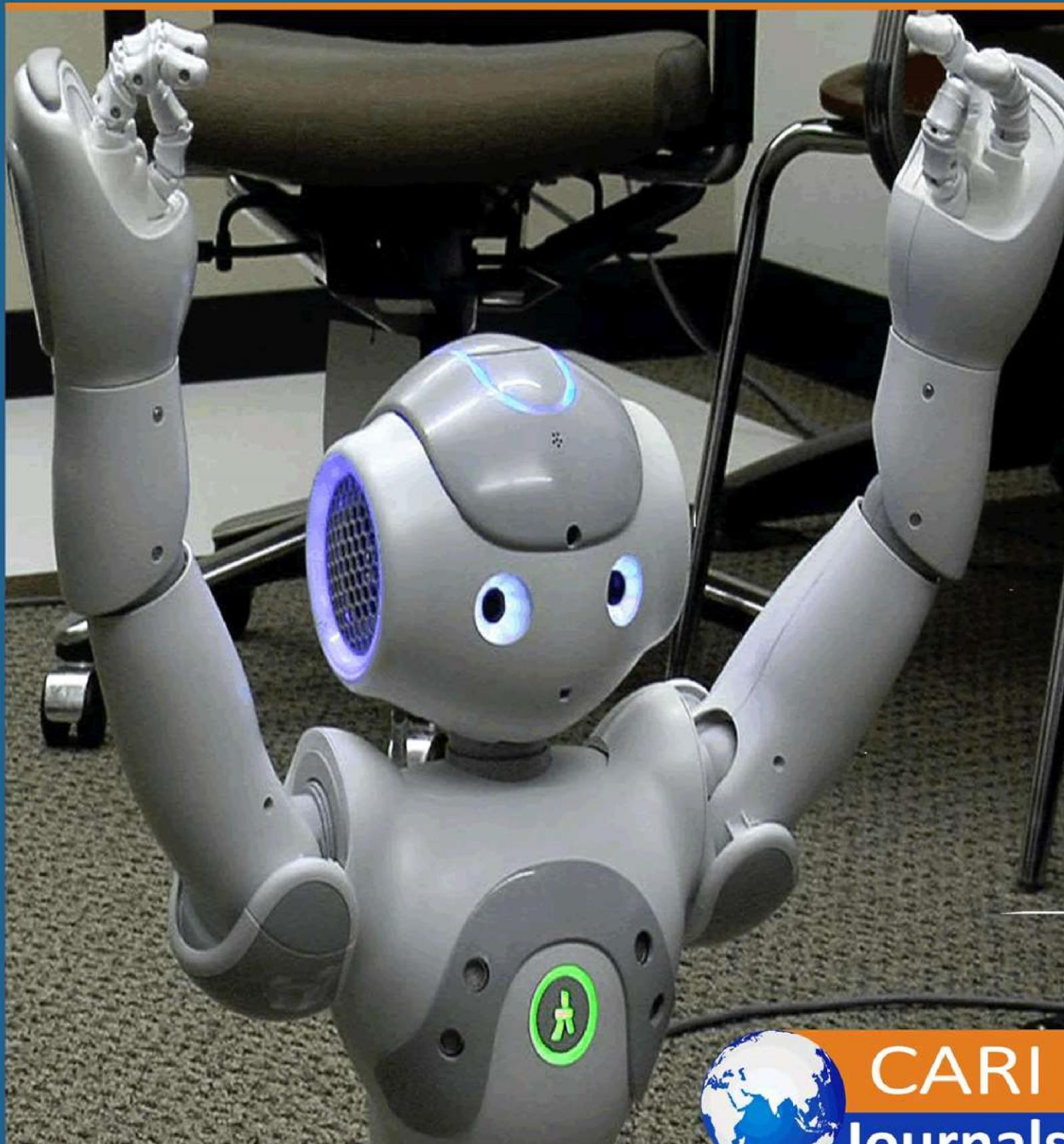

CARI
Journals

International Journal of Computing and Engineering
ISSN 2958-7425 (online)
Vol. 6, Issue No. 7, pp. 12 - 26, 2024
www.carijournals.org

CFD Simulation of Steady, Compressible Flow around the Naca 2412 Airfoil

Stanley A. Omenai
Department of Mechanical Engineering, Mississippi State University, USA.
omenai@yahoo.com
https://orcid.org/0009-0000-8176-0906

Accepted: 30th Oct, 2024, Received in Revised Form: 14th Nov, 2024, Published: 21st Dec, 2024

Abstract

Purpose: The study of fluids is key for understanding the world around us. Today, aircrafts are ubiquitous for transportation of goods and personnel. The key forces at play during aircraft propulsion; lift and drag, are affected by the shape and positioning of the airfoils around the aircraft. Understanding of the flow dynamics around the airfoil in an aircraft is vital to optimizing its design.

Methodology: In this study, analysis of the NACA 2412 airfoil is carried out using ANSYS Fluent. A 2D model of the airfoil in a rectangular flow domain is developed, with air as the working fluid. The viscous-inviscid fluid model is assumed. Pressure-based solver type is adopted, with absolute velocity formulation and steady time. The pressure, density, velocity and Mach number behaviours at two different velocities and angles of attack respectively are then analysed.

Findings: At velocity magnitude of 285 m/s, there is a gradual change in fluid properties (pressure and density) after the leading edge, and a sharp change in the fluid properties towards the trailing edge of the airfoil. The former signifies the formation of expansion waves while the latter signifies the formation of shock waves. The flow after the stagnation point also moves gradually from subsonic to supersonic upstream of the shock wave, and abruptly to subsonic after the shock wave. This indicates that as freestream velocity approaches the speed of sound, there is increased tendency for the formation of expansion and shock waves. The nature and location of the waves depend on the angle of attack of the airfoil.

Unique Contribution to Theory, Practice and Policy: The analysis results provide significant insights into the aerodynamic behaviour of airfoils under different flight conditions, providing a more cost-effective solution for aircraft design optimization, compared to using models in wind tunnels at the early design stages.

Keywords: *NACA 2412 Airfoil, CFD, Compressible Flow, Shock Wave, Expansion Wave, Angle of Attack, ANSYS Fluent*

International Journal of Computing and Engineering
ISSN 2958-7425 (online)
Vol. 6, Issue No. 7, pp. 12 - 26, 2024
www.carijournals.org

INTRODUCTION

In our world today, aircrafts are commonplace for transportation of goods and personnel. The key forces at play during aircraft propulsion; lift and drag, are affected by the shape and positioning of the airfoils around the aircraft. Understanding of the flow dynamics around the airfoil at different velocities and angles of attack is thus vital to optimizing aircraft design.

In the past, study of fluid flow was done using models in wind tunnels. With advancement in technology and development of Computational Fluid Dynamics (CFD) techniques, several fluid flow simulation softwares have become available, thus, making the process more cost effective and requiring minimal laboratory work.

The NACA 2412 airfoil, developed by the National Advisory Committee for Aeronautics (NACA), has been extensively studied for its aerodynamic characteristics. Its cambered structure and smooth curvature make it a preferred choice for low to medium-speed airfoil applications, such as aircraft wings, wind turbine blades, and UAVs [1]. Understanding the behaviour of compressible flow around such airfoils is essential during design for optimizing aerodynamic performance.

Steady compressible flow studies focus on Mach numbers where the flow transitions to compressible regimes (typically beyond 0.3 Mach). Accurate prediction of flow parameters such as pressure distribution, shock waves, and separation points requires robust CFD tools.

Problem Statement

While experimental data on NACA 2412 airfoil behaviour under incompressible and low-speed flow conditions is well-documented, there is a lack of comprehensive numerical analysis for steady compressible flow regimes where significant changes in density occur. Compressible flows, often associated with transonic and supersonic speeds, introduce additional complexities such as shock and expansion waves, which affect the aerodynamic performance of the airfoil.

Numerical simulations using CFD provide an efficient approach to study the flow characteristics, pressure distribution, lift, drag, and shock/expansion waves formation around airfoils operating in compressible flow conditions. ANSYS Fluent, a widely adopted CFD software, offers robust solvers for steady compressible flow simulations. However, accurate modelling of flow physics around the NACA 2412 airfoil requires appropriate mesh resolution, and boundary conditions to capture compressibility effects and predict aerodynamic parameters with high accuracy.

Objective

The objective of this study is to conduct aerodynamic analysis on the NACA 2412 airfoil using ANSYS Fluent to understand the pressure, density, velocity and Mach number behaviours at different velocities and angles of attack.

International Journal of Computing and Engineering
ISSN 2958-7425 (online)
Vol. 6, Issue No. 7, pp. 12 - 26, 2024
www.carijournals.org

Methodology

Analysis of the NACA 2412 airfoil with chord length of 1m is conducted. A 2D model of the airfoil in a rectangular flow domain is developed, with air as the working fluid. Quadrilateral elements are used for meshing. The viscous-inviscid fluid model is assumed. Pressure-based solver type is adopted, with absolute velocity formulation and steady time. The pressure, density, velocity and Mach number behaviours at two different velocities and angles of attack respectively are then analysed.

The analysis shows that as freestream velocity approaches the speed of sound, there is increased tendency for the formation of expansion and shock waves. The nature and location of the waves depend on the angle of attack of the airfoil.

The results of this analysis can be further improved on by considering the airfoil sections for a complete aircraft rotor. A 3-dimensional propeller can be modelled by stacking up all the component airfoil sections and analysing using ANSYS Fluent or other commercial CFD softwares.

LITERATURE REVIEW

Introductory Concepts

The motion of any fluid is governed by the Navier-Stoke's equations. For 2D airfoils, using a coordinate system placed on the surface of the airfoil, only two components of the velocity are considered: normal (y-axis) and tangential (x-axis) velocities. The velocity component on the spanwise direction (z-axis) is considered to be zero [2].

The effect of this velocity generates a distribution of pressure on upper and lower surfaces of the airfoil that cause vertical and horizontal forces on the airfoil profile [2]. The reacting force F from the flow is decomposed into a direction perpendicular to the velocity at infinity V_∞, and to a direction parallel to V_∞. The former component is known as lift (L) and the latter is called drag (D).

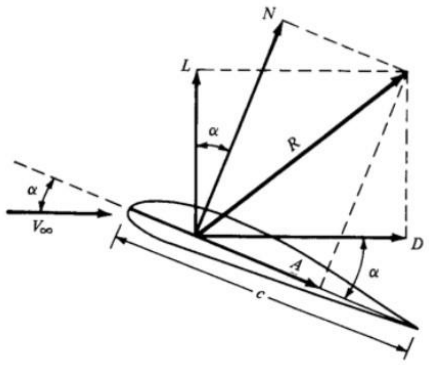

Figure 1: Lift and Drag forces on an airfoil [2].

- c is the chord of the airfoil profile and V_∞ is the freestream wind velocity
- α is the angle of attack (AOA) defined as the angle between the chord-line and V_∞

- Re is the Reynolds number based on the chord, c and the flow speed V_∞
- Ma denotes the Mach number, defined as the ratio between the flow speed and the speed of sound.

Inviscid flow is the flow of an inviscid (zero-viscosity) fluid with Reynolds number approaching infinity as the viscosity approaches zero. Inviscid flow results in slip boundary conditions [3].

The Euler equations are a set of quasilinear partial differential equations governing adiabatic and inviscid flow [2]. They correspond to the Navier–Stokes equations with zero viscosity and zero thermal conductivity. The Euler equations can be applied to incompressible or compressible flow. The compressible Euler equations consist of equations for conservation of mass, balance of momentum, and balance of energy, together with a suitable constitutive equation for the specific energy density of the fluid [2].

Ludwig Prandtl developed the modern concept of the boundary layer. His hypothesis established that for fluids of low viscosity, shear forces due to viscosity are evident only in thin regions at the boundary of the fluid, adjacent to solid surfaces. Outside these regions, and in regions of favourable pressure gradient, viscous shear forces are absent so the fluid flow field can be assumed to be the same as the flow of an inviscid fluid [3].

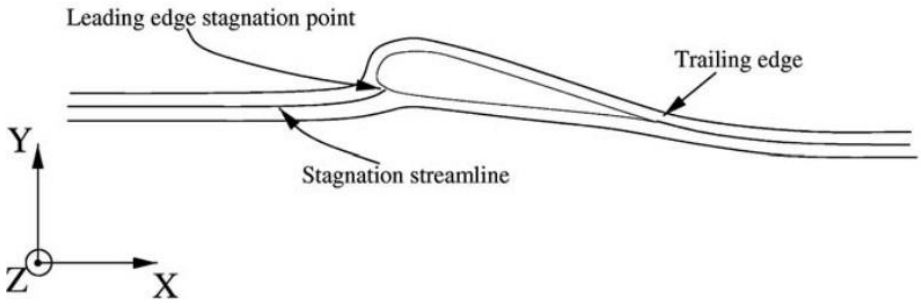

Figure 2: Flow over 2D airfoil [2].

For non-ideal flows and bodies with curvature, boundary layer separates at some point of the surface of interest. At the separation point, a vortex sheet is generated, and potential flow solutions are no longer valid.

A shock wave is a type of propagating disturbance that moves faster than the local speed of sound in the medium [4]. Like an ordinary wave, a shock wave carries energy and can propagate through a medium but is characterized by an abrupt, nearly discontinuous, change in pressure, temperature, and density of the medium. Shock waves could be of three forms: normal, oblique or bow [4]. Normal shocks are compressed waves oriented such that the wave front is perpendicular to the flow direction. Oblique shocks are inclined to the flow direction. They occur when the flow is deflected by a concave corner and is forced to turn into itself. Bow shocks are curved detached shocks observed in front of blunt bodies. These can be visualized as a superposition of both normal and oblique shocks.

International Journal of Computing and Engineering
ISSN 2958-7425 (online)
Vol. 6, Issue No. 7, pp. 12 - 26, 2024
www.carijournals.org

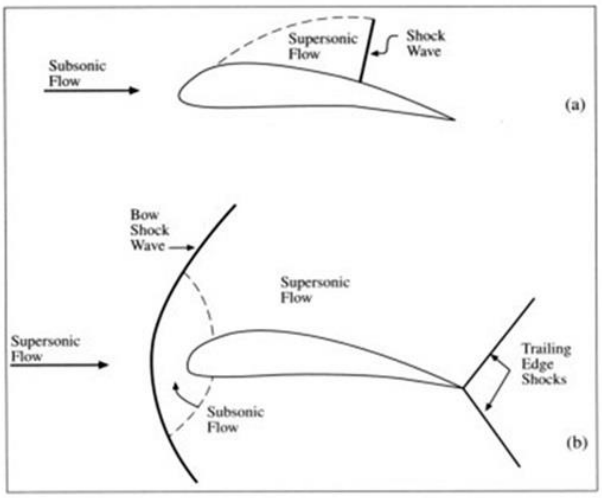

Figure 3: Transonic flow over an airfoil. (a) Freestream flow slightly below the speed of sound (Mach number from 0.8 to 0.9). (b) Freestream flow slightly above the speed of sound (Mach number from 1.0 to 1.2) [4].

Expansion waves in supersonic flows are formed when the flow area suddenly expands [4]. This happens when the flow encounters a convex corner. The expansion region is continuous in that the properties vary relatively smoothly and continuously, which is opposite to the abrupt change across a shock. The expansion process has the effect of increasing the Mach number (flow accelerates) and decreasing static flow properties (pressure, temperature, and density) [4].

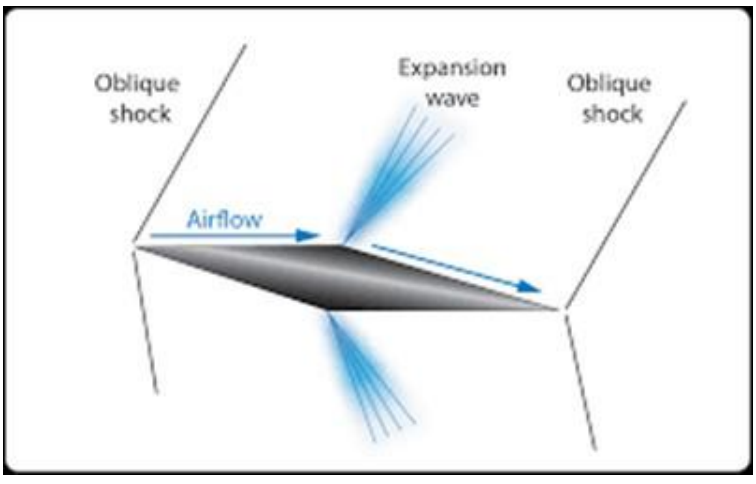

Figure 4: Oblique Shock and Expansion waves [4].

Shock and expansions seldom occur in isolation. They interact with themselves or with their surrounding environments (such as walls) [4].

Shock waves create a high-pressure region in front of an airfoil and a low-pressure region behind it. This pressure difference reduces the net force that pushes it forward [4].

A shock wave can limit the maximum speed of an aircraft as for each airfoil there is a critical Mach number which is associated with the onset of a sharp rise of the drag coefficient [4]. This is due to the wave drag which increases as the shock grows stronger. As a result of this, to obtain a higher value (i.e., increase maximum speed for same power or have the same speed for less fuel consumption) supercritical airfoils are used for transport aircrafts which employ a rather flat upper surface to delay and attenuate shock [4].

Anderson, J. D. discussed the behaviour of compressible flows, and detailed how shock waves and expansion fans form as flow accelerates and decelerates over aerodynamic surfaces like airfoils [5]. The influence of the angle of attack on the location and strength of shock waves was also highlighted.

Use of Computational Fluid Dynamics (CFD) Analysis in Design

Computational Fluid Dynamics (CFD) has revolutionized the design process across various engineering fields by providing a detailed understanding of fluid flow behaviour, heat transfer, and associated phenomena.

CFD enables engineers to evaluate multiple design iterations rapidly during the conceptual phase without the need for physical prototypes. For instance, in aerodynamic design, CFD is extensively used to optimize airfoil shapes, vehicle aerodynamics, and turbine blades. Studies, such as by Versteeg and Malalasekera [6], highlight how CFD reduces reliance on wind tunnel tests and accelerates development timelines.

CFD eliminates or reduces the need for expensive experimental setups by simulating complex fluid flows virtually. For example, Roache [7] emphasizes that CFD allows engineers to test extreme operating conditions that might be infeasible or risky in real life.

CFD is tailored for various industries such as aerospace, automotive, energy, and biomedical engineering. In renewable energy, it has been used to model multiphase flows in wind turbines and hydrodynamic performance in wave energy converters [8].

By leveraging CFD analysis, designers can address challenges efficiently, enhancing innovation and performance while reducing cost and time-to-market.

Previous CFD Studies on the Naca 2412 Airfoil

Several researchers have conducted experimental and numerical studies to investigate the aerodynamic characteristics of the NACA 2412 airfoil under different flow regimes. An aerodynamic study of the air flow effect around different NACA 2412 airfoil geometries was performed by Rashid et al [9] using methods of CFD. The simulation was done by solving the governing equations (Continuity, Reynolds Averaging Navier-Stokes and Energy Equation) in 2-D using ANSYS Fluent at Reynolds number of 10^6. The forces of lift and drag were observed to increase with increasing angle of attack till reaching stall.

Samuel et al [10] evaluated the performance of surface-modified NACA 2412 airfoil with variable cavity characteristics such as size, shape and orientation. It was observed that the

aerodynamic efficiency of cavity airfoil was improved by enhancing the maximum lift to drag ratio with delayed flow separation even at higher angle of attack.

CFD simulation of steady state flow around the NACA 2412 airfoil with 230 mm chord length at 30m/s from 0 to 16 angle of attack was conducted by Samuel et al [11]. The study provided insight on the flow behavior around the airfoil in the flow separation region.

Rao et al [12] performed numerical simulations on the NACA 2412 airfoil at subsonic speeds using ANSYS Fluent. The study emphasized the importance of grid independence, turbulence models, and solver accuracy.

Venkatesh et al investigated the effect of compressibility on flow characteristics of cambered airfoils [13]. They found that shock waves begin to form at Mach numbers close to 0.7, which significantly increases drag and alters lift performance.

Yin et al focused on steady-state simulations of compressible flow around NACA airfoils [14]. Their research highlighted the role of mesh refinement near the leading edge and trailing edge for capturing shocks and separation points accurately.

Hassan et al explored the challenges of shock wave formation at higher Mach numbers, resolution of the laminar-to-turbulent transition in boundary layers and minimization of numerical dissipation to avoid smoothing out shocks and sharp gradients and recommended higher-order schemes and adaptive meshing techniques for better shock capturing [15].

This review underscores the need for continued research in refining numerical techniques to address challenges associated with compressible flows around airfoils.

Problem Setup

Geometry

The DAT file of NACA 2412 airfoil available on the NACA website was used. The file contains the coordinates of the vertices from which the airfoil profile is formed. The airfoil has its leading edge at x=0, and chord equal to 1m.

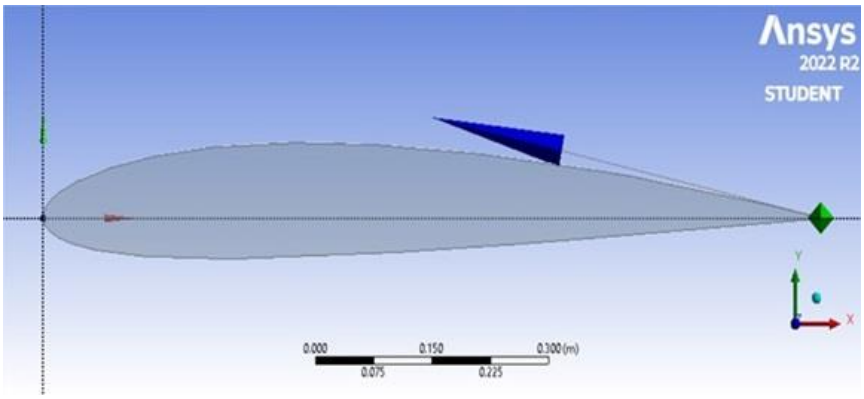

Figure 5: Profile of airfoil.

The DAT file contains only vertices coordinates; hence we need to create a control volume around the airfoil to analyse the flow. We achieve this by defining a 2D rectangular flow

domain, extending from -4 to 8 in the x-direction and from -4 to 4 in the y-direction. The rectangular domain is further split into six (6) different faces to help in the mesh refinement process. This will enable us to mesh each face separately and accurately capture the flow physics within each region.

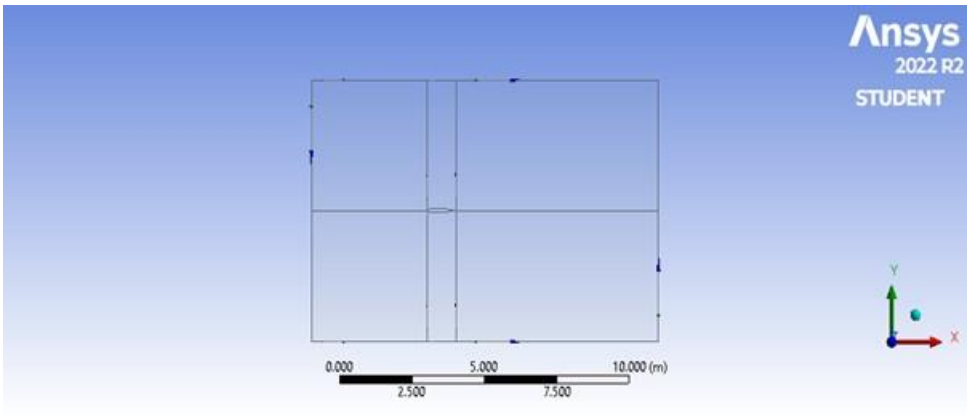

Figure 6: Airfoil within rectangular flow domain split into six faces.

Meshing

Quadrilateral elements are used for the 2D meshing of the control volume in ANSYS Fluent Mesh module. The mesh at the region around the airfoil and the flow field is refined to correctly capture the flow physics around those regions. The edge sizing for the mesh faces is refined using number of divisions and allowing for bias towards the airfoil location. High mesh resolution is obtained around the airfoil while low mesh resolution is obtained on the farfield boundaries.

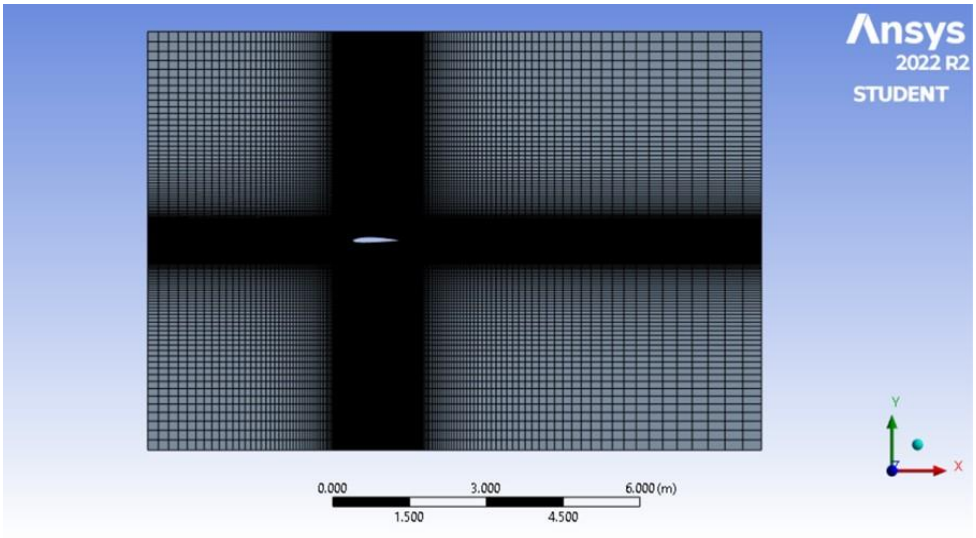

Figure 7: Mesh of control volume generated.

Material Properties

The rectangular control volume is a fluid domain while the airfoil is considered as a wall within the fluid domain. The material of the airfoil is irrelevant in this case as it is a solid wall. The fluid is air, considered as a compressible, ideal gas, with constant specific heat capacity and molecular weight.

Table 1: Properties of Air

Material	Property	Value
Air	Density	Ideal Gas
	Specific Heat Capacity	1006.43 J/kgK
	Molecular Weight	28.966 kg/kmol

Boundary Conditions

The boundary conditions are applied to the surface of the airfoil and the four (4) sides of the rectangular flow domain.

I. In the case of 0° angle of attack, the following boundary conditions are applied:

Table 2: Boundary conditions for 0° angle of attack and 200m/s Velocity

Boundary Field	Boundary Condition	Type	Value
Inlet	Velocity	Velocity Components	(200,0) m/s
Outlet	Pressure	Gauge Pressure	0 barg
Top	Velocity	Velocity Components	(200,0) m/s
Bottom	Velocity	Velocity Components	(200,0) m/s
Airfoil	Wall	Fixed	N/A

Table 3: Boundary conditions for 0° angle of attack and 285m/s Velocity

Boundary Field	Boundary Condition	Type	Value
Inlet	Velocity	Velocity Components	(285,0) m/s
Outlet	Pressure	Gauge Pressure	0 barg
Top	Velocity	Velocity Components	(285,0) m/s
Bottom	Velocity	Velocity Components	(285,0) m/s
Airfoil	Wall	Fixed	N/A

II. In the case of 5° angle of attack, the top side of the flow domain is a pressure outlet since flow exits the domain from the top due to the direction of flow imposed by the angle of attack. The velocity components are obtained from the velocity magnitude, *v*, using the following relations:

$$v_x = v\cos\alpha\,; \quad v_y = v\sin\alpha$$

The following boundary conditions are applied:

Table 4: Boundary conditions for 5° angle of attack and 200m/s Velocity

Boundary Field	Boundary Condition	Type	Value
Inlet	Velocity	Velocity Components	(199.24,17.43) m/s
Outlet	Pressure	Gauge Pressure	0 barg
Top	Pressure	Gauge Pressure	0 barg
Bottom	Velocity	Velocity Components	(199.24,17.43) m/s
Airfoil	Wall	Fixed	N/A

Table 5: Boundary conditions for 5° angle of attack and 285m/s Velocity

Boundary Field	Boundary Condition	Type	Value
Inlet	Velocity	Velocity Components	(283.92,24.84) m/s
Outlet	Pressure	Gauge Pressure	0 barg
Top	Pressure	Gauge Pressure	0 barg
Bottom	Velocity	Velocity Components	(283.92,24.84) m/s
Airfoil	Wall	Fixed	N/A

Processing

Pressure-based solver type is adopted, with absolute velocity formulation, steady time and planar 2D space. The fluid model used is the viscous-inviscid type. The energy equation is solved since the inviscid Euler equations include Energy. The coupled pressure-velocity coupling scheme is adopted with least squares cell-based gradient spatial discretization. Second order pressure discretization is used, while second order upwind discretization is used for the density, momentum, and energy equations. Flow Courant number of 5 is used to control the solution. Standard initialization method is used, with flow computed from the inlet. The final

step is the solution step. This involves solving the problem using the calculate command. Once the solution has converged, the results are viewed in ANSYS Fluent.

RESULTS AND DISCUSSIONS

The following profiles were obtained from the initial case using angle of attack of 0° at an inlet velocity of magnitude 200 m/s.

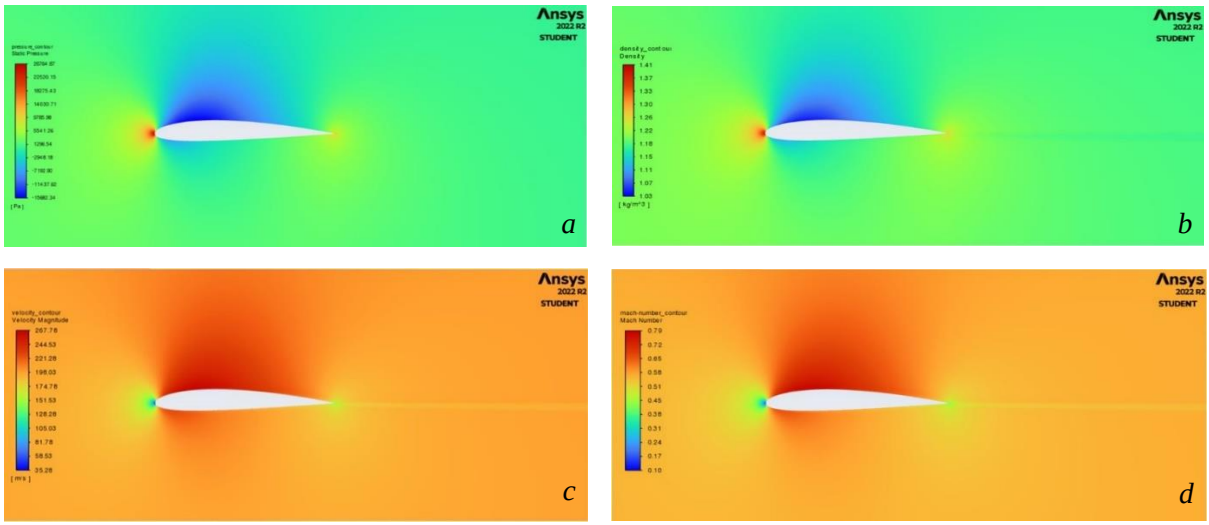

Figure 8: (a) Pressure, (b) Density, (c) Velocity and (d) Mach number variation around airfoil at 200m/s and 0° AOA

The following profiles were obtained from the same case with angle of attack of 0° at an inlet velocity of magnitude 285 m/s.

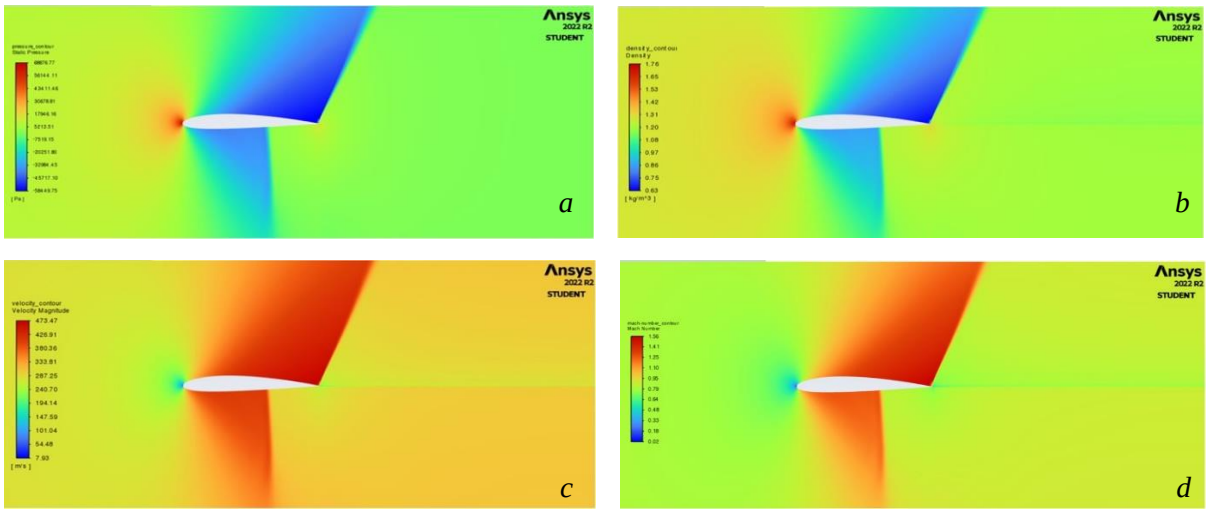

Figure 9: (a) Pressure, (b) Density, (c) Velocity and (d) Mach number variation around airfoil at 285m/s and 0° AOA

From fig. 8 (a), we observe a reduction in pressure above the airfoil after the leading edge, while the pressure below remains nearly same. This provides a differential pressure in the upward direction, generating lift on the airfoil.

Fig. 8 (c) shows the increased flow velocity above the airfoil after the leading edge. This is consistent with the Bernoulli's principle as increased flow velocity leads to reduction in pressure. Also, at the leading edge of the airfoil, we note significant pressure build-up and velocity reduction. This is a stagnation point.

Fig. 8 (d) shows an increase in Mach number in the region above the aircraft. However, the flow is still within the subsonic region.

In fig. 9 (a) & (b), we see a gradual change in fluid properties (pressure and density) after the leading edge, and a sharp change in the fluid properties towards the trailing edge of the airfoil at the top and bottom sections. The former signifies the formation of expansion waves while the latter signifies the formation of shock waves. The shock waves are perpendicular to the surface of the airfoil, hence, they are normal shock waves.

From fig. 9 (d), we observe from the Mach number that there is stagnation at the leading edge, thereafter, the flow moves gradually from subsonic to supersonic upstream of the shock wave, and abruptly to subsonic after the shock wave.

The following profiles were obtained from the second case using angle of attack of 5° at an inlet velocity of magnitude 200 m/s.

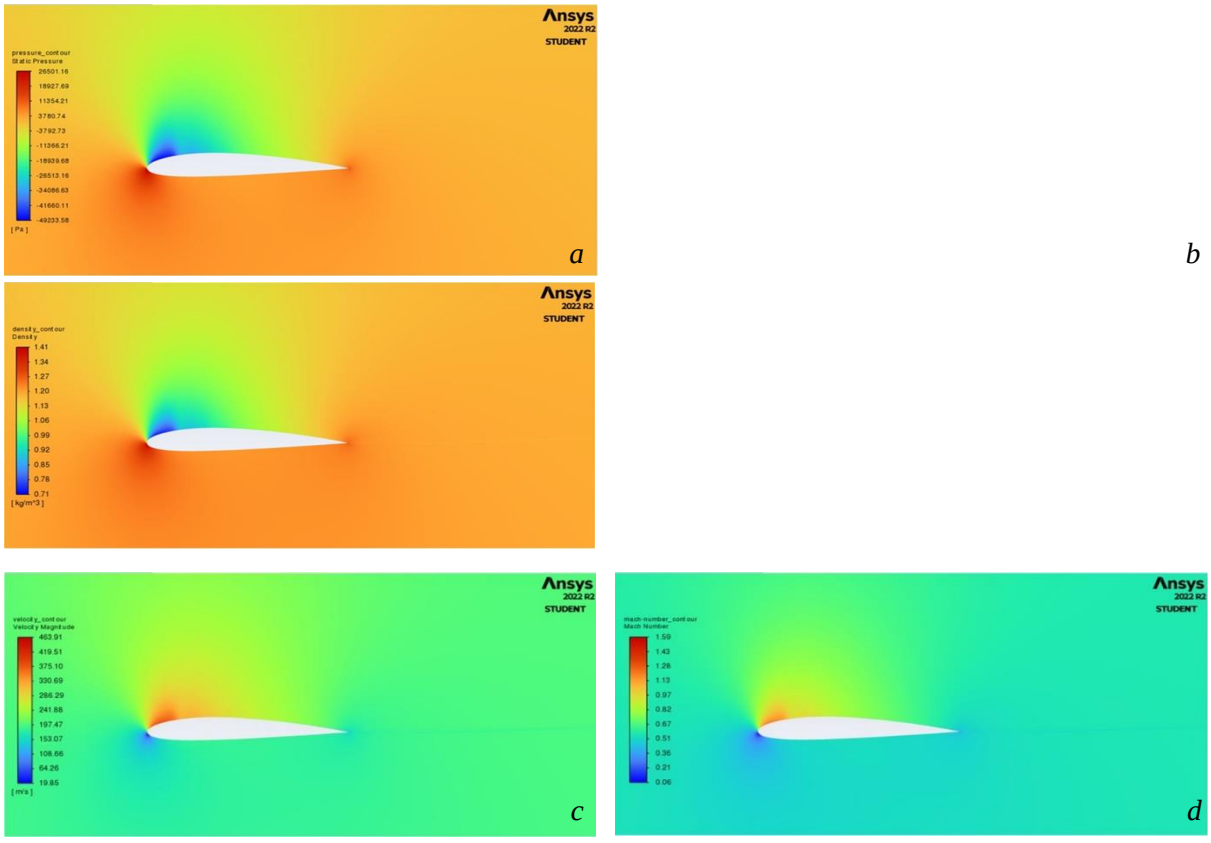

Figure 10: (a) Pressure, (b) Density, (c) Velocity and (d) Mach number variation around airfoil at 200m/s and 5° AOA

International Journal of Computing and Engineering
ISSN 2958-7425 (online)
Vol. 6, Issue No. 7, pp. 12 - 26, 2024
www.carijournals.org

The following profiles were obtained from the same case with angle of attack of 5° at an inlet velocity of magnitude 285 m/s.

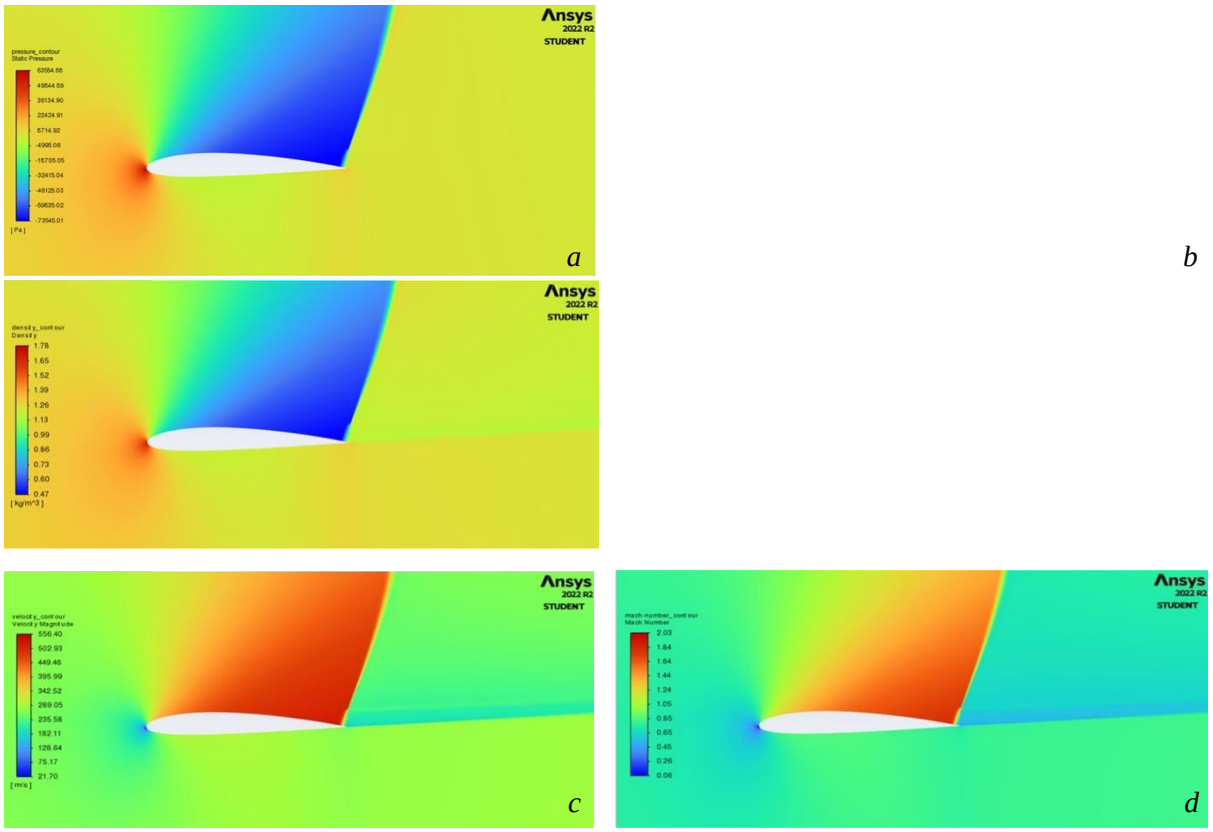

Figure 11: (a) Pressure, (b) Density, (c) Velocity and (d) Mach number variation around airfoil at 285m/s and 5° AOA

In this case, we observe from fig. 10 (a) that the pressure variation was prominent at the upper part of the airfoil, towards the leading edge.

From fig. 10 (c), there is a sharp increase in the flow velocity just after the leading edge of the airfoil, which gradually decreases towards the trailing edge.

Also, at the leading edge of the airfoil, we note significant pressure build-up and velocity reduction. This is a stagnation point.

In figs. 11 (a) and (b), we see a gradual change in fluid properties (pressure and density) after the leading edge, and a sharp change in the fluid properties towards the trailing edge of the airfoil at the top section only. The former signifies the formation of expansion wave while the latter signifies the formation of a normal shock wave at this section.

From fig. 11 (d), we observe from the Mach number that there is stagnation at the leading edge, thereafter, the flow moves gradually from subsonic to supersonic upstream of the shock wave, and abruptly to subsonic after the shock wave.

In our analysis, we observe a reduction in pressure and increased flow velocity over the upper surface of the airfoil after the leading edge for all the cases. This leads to generation of lift and

is consistent with the Bernoulli principle. Also, at the leading edge of the airfoil, we note significant pressure build-up and velocity reduction. This is a stagnation point.

At velocity magnitude of 285 m/s for both cases, we see a gradual change in fluid properties (pressure and density) after the leading edge, and a sharp change in the fluid properties towards the trailing edge of the airfoil. The former signifies the formation of expansion waves while the latter signifies the formation of of shock waves. The shock waves are perpendicular to the surface of the airfoil, hence, they are normal shock waves.

We observe from the Mach number plots, that the expansion and shock waves begin to form at Mach number of approximately 0.7. Also, flow after the stagnation point moves gradually from subsonic to supersonic upstream of the shock wave, and abruptly to subsonic after the shock wave.

The study coroborates the result of previous studies. Venkatesh et al investigated the effect of compressibility on flow characteristics of cambered airfoils [12] and found that shock waves begin to form at Mach numbers close to 0.7.

From this analysis, we can conclude that as freestream velocity approaches the speed of sound, there is increased tendency for the formation of expansion and shock waves. The nature and location of the waves depend on the angle of attack of the airfoil. This is consistent with the behavior of compressible flows, particularly in the transonic regime, as espoused by Anderson, J. D. in *Fundamentals of Aerodynamics* [5].

CONCLUSION

This study provides valuable insights into the aerodynamic performance of the NACA 2412 airfoil under different flow conditions. The analysis successfully demonstrated the ability of CFD to capture critical flow characteristics such as pressure distribution and velocity profiles. The simulation highlighted the expected pressure variations along the airfoil's surface, with a lower pressure region forming on the upper surface due to higher velocity, consistent with Bernoulli's principle. For higher Mach numbers, the simulation captured compressibility effects, including the formation of expansion and shock waves, which significantly impacts aerodynamic behaviour. The study underscores the capability of ANSYS Fluent to model compressible flows effectively, providing engineers with a robust tool for airfoil design and optimization.

RECOMMENDATION

This analysis assumes steady-state conditions and neglects potential unsteady phenomena such as flow separation or vortex shedding, which could be explored in future work. Extending the study to transient simulations or incorporating turbulence modelling could provide further insights into the real-world aerodynamic behaviour of the airfoil. The results of this analysis can be further improved on by considering the airfoil sections for a complete aircraft rotor. A 3-dimensional propeller can be modelled by stacking up all the component airfoil sections and analysing using ANSYS Fluent or other commercial CFD software.

REFERENCES

1. Abbott, I. H., Doenhoff, A. E. von. (1959). *Theory of Wing Sections*. Dover Publications.
2. E., Stewart, Warren; N., Lightfoot, Edwin (2007). *Transport phenomena*. Wiley.
3. Streeter, Victor L. *(1966) Fluid Mechanics, 4th edition,* McGraw-Hill Book Co.
4. ANSYS Innovation Courses; *Introduction to Applications of Shock-Expansion Theory (2020);* ANSYS Inc.
5. Anderson, J. D. (2010). *Fundamentals of Aerodynamics.* McGraw-Hill Education
6. Versteeg, H. K., Malalasekera, W. (2007). *An Introduction to Computational Fluid Dynamics: The Finite Volume Method*. Pearson Education
7. Roache, P. J. (1998). *Verification and Validation in Computational Science and Engineering*. Hermosa Publishers.
8. Ferziger, J. H., Perić, M. (2002). *Computational Methods for Fluid Dynamics*. Springer.
9. Rashid, F., Abd, H., Hussein, E. (2022). *Numerical study of the air flow over modified NACA 2412 airfoil using CFD*. AIP Conference Proceedings. 2415. 20005. 10.1063/5.0092303.
10. Samuel, M., Rajendran, P., Khan, S. (2022). *CFD Simulation of NACA 2412 airfoil with new cavity shapes*. Advances in Aircraft and Spacecraft Science. 9. 131-148. 10.12989/aas.2022.9.2.131.
11. Samuel, M., Rajendran, P. (2019). *CFD Validation of NACA 2412 Airfoil.* 10.13140/RG.2.2.16245.42723.
12. Rao, A., Reddy, S. M., Sharma, K. (2017). *Turbulence model comparison for NACA airfoils at high Mach numbers*. Journal of Fluid Mechanics Research, 45(3), 325-338. https://doi.org/10.1016/j.jfluidmechres.2017.02.012
13. Venkatesh, K., Babu, V. (2019). *Effect of compressibility on flow characteristics around NACA 2412 airfoil*. Aerospace Science and Technology, 85, 450-459. https://doi.org/10.1016/j.ast.2019.02.014
14. Yin, H., Zhang, P., Wu, T. (2020). *Steady compressible flow simulation and analysis of NACA airfoils using high-resolution meshes*. Computers & Fluids, 200, 104426. https://doi.org/10.1016/j.compfluid.2020.104426
15. Hassan, M. S., Ali, R. N., Zhang, L. (2022). *Numerical investigation of shock wave effects on aerodynamic performance of NACA 2412 airfoil.* International Journal of Aerodynamics, 12(1), 78-92. https://doi.org/10.1504/IJA.2022.123456